calculations are reported; this paper addresses several points treated here. The reaction profile for the hydration of carbon dioxide and active solvation of bicarbonate bound to zinc has striking similarities to ours. The geometry of their structure **28** resembles our saddle point **B4**. For active solvation, their structure **35** looks also similar to our **C2t**. The activation barriers obtained with AM1 are, however, rather large.

When the present structural data are compared to those obtained with AM1, it appears that this particular empirical method is fairly successful in rendering transition structures for the interconversion process. This is good news since computing costs are unbearable when ab initio calculations are carried out at the level of basis set enterprised here. Unfortunately, the energetics of AM1 for the reaction profiles is profoundly at variance with our calculations and those by Pullman's group. The difference concerns both the shape of the energy profiles and activation barriers. The actual shape of the hypersurface for this type of reaction is essential for describing the molecular mechanism.

The mechanistic role of zinc in carbonic anhydrases appears to be rather complex. Hydroxide bound to zinc becomes a poor nucleophile. The carbonyl function must be activated before a nucleophilic attack (hydroxylation) may take place. The present theoretical results provide a fairly different picture of nucleophilicity when compared to the standard model.[1,4,6-8,9b] For the molecular events occurring at the level of the zinc coordination shell in the enzyme during interconversion, we suggest, as a hypothesis, that the corresponding energy profile has an inverted shape where the energy difference between **R** and **P** (cf. Figure 6) is controlled by surrounding medium effects.[70-72]

Acknowledgment. Olivier Jacob gratefully acknowledges financial support from Merrell Dow Research Institute. Orlando Tapia thanks the Swedish Research Council for financial assistance. We are grateful to Mons Ehrenberg from BMC, who also got into the inverted profile hypothesis from a completely different path, for invaluable discussions. We thank Profs. S. Lindskog, E. M. Evleth, and R. Bywater for reading the manuscript and for giving us helpful advice. We are also indebted for the constructive comments from the referees.

Registry No. CO_2, 124-38-9; $Zn(OH)^+$, 22569-48-8; $Zn(NH_3)_3OH^+$, 72147-20-7.

(69) Merz, K. M., Jr.; Hoffman, R.; Dewar, M. J. S. *J. Am. Chem. Soc.* **1989**, *111*, 5636.

(70) The energy difference between **R** and **P** may be modulated by enzyme and solvent effects[40,71,72] because the product, bicarbonate zinc ion, has an ion-pair nature, while the reactant is a neutral molecule interacting with an ion; consequently, the energy difference between reactant and product can be reduced and fine tuned by the enzyme system.[40,72] Now, for an inverted type of energy profile, the kinetics are determined by the energy difference between reactants and products, while differential kinetic efficiency among isozymes would be dependent upon the detailed path for interconversion at the bottom of the well. Experimental and theoretical work on inverted potential energy shape for gas-phase nucleophilic displacement reactions[17] and carbo-acid strength[16] have documented such behavior. Consequently, the rate-limiting step for the reaction must be found at the other stages of the mechanism depicted in Scheme II.[1,3,4]

(71) Sheridan, R. P.; Allen, L. C. *J. Am. Chem. Soc.* **1981**, *103*, 1544.

(72) (a) Warshel, A.; Sussman, F. *Proc. Natl. Acad. Sci. U.S.A.* **1986**, *83*, 3806. (b) Warshel, A.; Weiss, R. *J. Am. Chem. Soc.* **1980**, *102*, 6218.

Electronic Structure of Icosahedral Cobalt-Sulfur Clusters

Gary G. Hoffman,† James K. Bashkin,‡ and Martin Karplus*

Contribution from the Department of Chemistry, Harvard University, Cambridge, Massachusetts 02138. *Received January 22, 1990*

Abstract: This paper uses the multiple scattering (MS)-Xα method to calculate the electronic structure of several clusters that contain an octahedral Co_8S_6 core. Two of the clusters are analogous to compounds that have been previously synthesized, and the results of these calculations are consistent with the experimentally observed spin states, absorption spectra, and structural similarity of these compounds. These clusters are of particular interest because they are related to the component structures of the mineral cobalt pentlandite. To obtain information that can be extended to cobalt pentlandite, the effects of oxidation state and added ligands to the core structure of the clusters are studied. An extended Hückel theory (EHT) study of similar clusters has been performed by Burdett and Miller. In addition to MS-Xα results, we present EHT calculations on clusters of lower symmetry than those studied by Burdett and Miller. The spectra from the two types of calculations correspond in general and the central conclusions of Burdett and Miller are supported by the MS-Xα results. However, because the MS-Xα calculations take account of the electron-electron interactions explicitly, they provide more rigorous information on the effects observed. Specifically, the cobalt-sulfur bonding orbitals are observed to form a separate lower energy band whose structure varies upon addition of ligands to the cluster, spin pairing is found not to be important in determining the ground-state configurations, and the tendency of the cluster to contract upon addition of ligands is found to be due to an overall redistribution of charge rather than to any specific orbitals.

1. Introduction

Metal sulfide minerals offer a wide variety of structures, some with "extraordinary physical properties"[1] that stem from the fact that they are extensively interconnected and are not decomposable into independent molecular building blocks. However, there exists a class of these compounds that is made up of extended lattices of recognizable metal sulfide clusters that are connected by bridging interactions. The most famous of these substances are probably the Chevrel phases of the molybdenum chalcogenides,[2] which have unusual conducting properties. Pentlandite is a

Table I. Average Bond Distances (Å)[a]

	$[Co_8S_6(SPh)_8]^{4-}$[b]		$[Co_8S_6(SPh)_8]^{5-}$[b]	pentlandite (Co_9S_8)[c]
	anion 1	anion 2		
Co-Co	2.662	2.653	2.674	2.505
Co-S_b	2.230	2.226	2.236	2.227
Co-S_t	2.239	2.242	2.276	2.127

[a] The bond lengths for the salts are average values, with the individual bond lengths differing by as much as 0.02 Å from the mean. [b] Reference 5. [c] Reference 30.

† Present address: Department of Chemistry, Florida International University, Miami FL 33199.

‡ NIH postdoctoral fellow, 1984-1985. Present address: Monsanto Co., 800 N. Lindbergh Boulevard, St. Louis, MO 63167.

0002-7863/90/1512-8705$02.50/0

naturally occurring mineral found as a composite of sulfides of several metals with the empirical formula $(Fe,Ni,Co)_9S_8$. It is possible to synthesize the pentlandite structure with cobalt as the only metal.[3] The crystal structure contains Co_8S_6 cluster units, each of which consists of a cubic arrangement of cobalt atoms whose faces are capped by the six sulfur atoms, the sulfur atoms alone forming an octahedron. These cluster units are joined to each other in a face-centered cubic array by bridging sulfur atoms that bond to the cobalt atoms of the clusters. In addition, the capping sulfur atoms of six neighboring, octahedrally oriented clusters bond to a centrally located cobalt atom. A more complete description of the crystal structure can be found elsewhere.[4]

Recently, salts of the clusters $[Co_8S_6(SPh)_8]^{4-,5-}$ have been synthesized[5] and the X-ray structures demonstrate that they have the same basic Co_8S_6 core as found in cobalt pentlandite. Two crystallographically independent clusters for the 4- salt and one for the 5- salt have been found. Comparison of mean bond lengths of the salts with each other and with the pentlandite structure is given in Table I. The $[Co_8S_6(SPh)_8]^{4-,5-}$ core structures differ from the pentlandite structure in that they have larger dimensions; the volume of the pentlandite Co_8S_6 core is only 81–84% of that occupied by the anionic species. After the phenyl groups are removed, the anions deviate only slightly from octahedral symmetry. There are two different types of sulfur atoms in these clusters, referred to here as *bridging* sulfurs for the sulfurs for the sulfurs contained in the Co_8S_6 core and *terminal* sulfurs for the sulfur atoms contained in the benzenethiolate ligands. The terminal sulfurs bond to the cobalt atoms and form a cube among themselves: they are analogous to the sulfurs that connect the Co_8S_6 clusters in pentlandite. The two anionic clusters have similar dimensions, but the reduced form is slightly larger and the cobalt to terminal sulfur bond is particularly long. The UV–vis absorption spectra of the two anionic species are very similar, each showing three major peaks. The 4- structure shows absorption bands at 253, 342, and 518 nm and the 5- structure has bands at 260, 348, and 488 nm. NMR spectra of the two salts are also very similar, and magnetic susceptibility measurements indicate that the structures have low-spin ground states, with $S = 0$ for 4- and $S = {}^1/_2$ for 5-.[5]

Assuming a formal charge of −2 for each sulfur, the average formal charge per cobalt atom is +2 for the 4- anion, +1.875 for the reduced 5- anion, and +1.75 for the hypothetical 6- anion. In the bulk Co_9S_8 material, if the octahedral Co atoms connecting the core clusters are assumed to have formal charges of +2, the average formal charge per cobalt atom in the core cluster is also +1.75; this suggests the closest similarity with the 6- anion. Thus, it is somewhat surprising that the pentlandite core in the crystal has shorter metal–metal bonds than the 4- or 5- model compounds. We examine this question, among others, in the calculations reported here.

One approach to model the electronic structure of these clusters is based on ligand field theory.[6] Each cobalt atom is placed in a tetrahedral field of S^{2-} ions, which splits the five cobalt d orbitals into a set of two e and three t_2 orbitals. The e orbitals are metal–ligand bonding while the t_2 orbitals are metal–ligand antibonding. If the metal–metal interactions were small, this picture could be extended to the Co_8S_6 cluster. If the interactions between the tetrahedral entities were small, the system would consist of 16 bonding orbitals and 24 antibonding orbitals. With seven d electrons contributed by each cobalt atom, all the bonding orbitals and 12 antibonding orbitals would be filled. Reduction of the 4- to the 5- cluster would require addition of an antibonding electron,

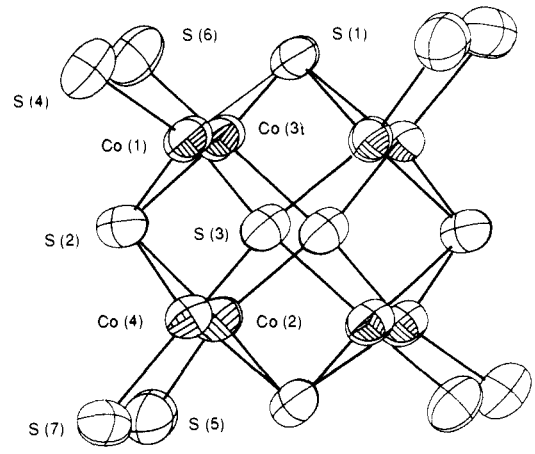

Figure 1. Co_8S_{14} core of these clusters.

which could be the cause of the expanded Co_8S_6 core. Moreover, ligand field theory assumes that the electrostatic interactions between the metal and ligand atoms are dominant. This is unjustified for the interconnected cluster considered here. Many of the ligands form bridges between the cobalt atoms and this leads to a situation where through-bond coupling is more important than the ligand field splittings.[7] In a study of the Co_2S_6 dimer that made use of extended Hückel theory, the inadequacy of ligand field theory and the complexity of the bonding in these complexes was demonstrated explicitly by Burdett and Miller.[8]

To supplement the extended Hückel calculations by a model that takes account explicitly of electron–electron interaction, we report multiple scattering (MS)–Xα[9] calculations for a series of structures containing the octahedral Co_8S_6 core. The anionic salts of $[Co_8S_6(SPh)_8]^{4-,5-}$ have been shown to deviate only slightly from octahedral symmetry, so that we can take advantage of the high symmetry of an idealized octahedral structure to simplify the calculation. Including the phenyl groups would require a substantial increase in the computation time, and since the properties of the core cluster are of primary interest, useful results can be obtained by either removing the phenyl groups or by substituting them with hydrogen atoms. The substitution of methyl groups for hydrogen atoms in Xα calculations for $Fe_4S_4(SH)_4^{2-}$ and in $Fe(SH)_4$ was observed to have little effect on the upper valence levels of the clusters.[10,11] Spin-restricted calculations were performed on the bare, octahedral symmetry $[Co_8S_{14}]^{12-}$ cluster to obtain a picture of the orbital structure due to the core while using relatively little computational effort. Protons were then added to the terminal sulfurs to mimic the effect of the phenyl groups in the salts and both spin-restricted and spin-polarized calculations were performed on this species. In the pentlandite crystal, there are ligands to the bridging sulfurs as well and the effect of these on the electronic structure was examined by adding protons at these sites of the cluster. Whether this is an important factor in the reduction of the Co_8S_6 core size in the crystal structure can be deduced by a comparison of the Hellmann–Feynman forces on the cobalt atoms in the structures with and without the hydrogen atoms bonded to the bridging sulfurs. The effect of adding electrons to the 4- structure, leading to the reduced 5- and 6- anions, was also studied. To aid in the interpretation of the Xα calculation, comparisons are made with the results of an extended Hückel treatment similar to that reported by Burdett and Miller.

Section 2 describes the methodology. The results are presented and discussed in Section 3. Section 4 outlines the conclusions.

(1) Wells, A. F. *Structural Inorganic Chemistry*, 3rd ed.; Clarendon Press: Oxford, England, 1962; p 511.
(2) Hughbanks, T.; Hoffmann, R. *J. Am. Chem. Soc.* **1983**, *105*, 1150–1162, and references therein.
(3) Pasquariello, D. M.; Kershaw, R.; Passaretti, J. D.; Dwight, K.; Wold, A. *Inorg. Chem.* **1984**, *23*, 872–874.
(4) Geller, S. *Acta Crystallogr.* **1962**, *15*, 1195–1198.
(5) Christou, G. K.; Hagen, S.; Bashkin, J. K.; Holm, R. H. *Inorg. Chem.* **1985**, *24*, 1010–1018.
(6) See, for example: Huheey, J. E. *Inorganic Chemistry*, 3rd ed.; Harper & Row: New York, 1983; pp 377–378.
(7) Summerville, R. H.; Hoffmann, R. *J. Am. Chem. Soc.* **1976**, *98*, 7240–7254.
(8) Burdett, J. K.; Miller, G. J. *J. Am. Chem. Soc.* **1987**, *109*, 4081–4091.
(9) Johnson, K. H. *Adv. Quantum Chem.* **1973**, *7*, 143–185.
(10) Aizman, A.; Case, D. A. *J. Am. Chem. Soc.* **1982**, *104*, 3269–3279.
(11) Norman, J. G., Jr.; Jackels, S. C. *J. Am. Chem. Soc.* **1975**, *97*, 3833–3835.

Table II. Model Geometries

	atomic coordinates (a_0)		
	x	y	z
outer sphere	0.0	0.0	0.0
Co	2.5118	2.5118	2.5118
	-2.5118	2.5118	2.5118
	2.5118	-2.5118	2.5118
	2.5118	2.5118	-2.5118
	-2.5118	-2.5118	2.5118
	-2.5118	2.5118	-2.5118
	2.5118	-2.5118	-2.5118
	-2.5118	-2.5118	-2.5118
S_b	4.7771	0.0	0.0
	0.0	4.7771	0.0
	0.0	0.0	4.7771
	-4.7771	0.0	0.0
	0.0	-4.7771	0.0
	0.0	0.0	-4.7771
S_t	4.9584	4.9584	4.9584
	-4.9584	4.9584	4.9584
	4.9584	-4.9584	4.9584
	4.9584	4.9584	-4.9584
	-4.9584	-4.9584	4.9584
	-4.9584	4.9584	-4.9584
	4.9584	-4.9584	-4.9584
	-4.9584	-4.9584	-4.9584
H_t	6.5753	6.5753	3.8057
	6.5753	6.5753	-3.8057
	6.5753	-6.5753	3.8057
	6.5753	-6.5753	-3.8057
	-6.5753	6.5753	3.8057
	-6.5753	6.5753	-3.8057
	-6.5753	-6.5753	3.8057
	-6.5753	-6.5753	-3.8057
H_b	7.3371	0.0	0.0
	0.0	7.3371	0.0
	0.0	0.0	7.3371
	-7.3371	0.0	0.0
	0.0	-7.3371	0.0
	0.0	0.0	-7.3371

	interatomic distances (a_0 (Å))		interatomic distances (a_0 (Å))
Co–Co	5.024 (2.658)	Co–S_t	4.238 (2.242)
Co–S_b	4.213 (2.220)	S–H	2.560 (1.350)

2. Methods

The extended Hückel and MS-Xα calculations are outlined. A picture of the Co_8S_{14} cluster is shown in Figure 1.

a. Extended Hückel Theory Calculations. Extended Hückel theory (EHT) calculations[12] were performed on a series of cobalt–sulfur clusters. These calculations treat only the valence levels and use input values for many of the Hamiltonian matrix elements, allowing qualitatively useful results to be obtained very little computational effort. The values for the matrix elements were obtained from the literature,[13] and the calculations were performed as described elsewhere.[14] The matrix elements were very slightly different from those used by Burdett and Miller[8] in their EHT calculations. However, the similarity in the results for compounds studied in both cases inplies that these diffrences are not significant.

All the EHT calculations used octahedrally symmetric arrangements of the Co_8S_{14} structure and had the following bond lengths: Co–Co, 2.6575 Å, Co–S_b, 2.2287 Å; Co–S_t, 2.2417 Å; S_t–H, 1.34 Å. These bond lengths are mean values of the average bond distances of the two anionic $[Co_8S_6(SH)_8]^{4-}$ clusters (see Table I). The S–H bond length is that of an organic thiol. The structure was built in steps from the Co_8^{16+} cube to the $[Co_8S_6(SH)_8]^{4-}$ cluster by adding the atoms according to their standard oxidation states, S^{2-} and H^+. The first calculation beyond the cobalt cube involves addition of six capping sulfurs. Next, the eight terminal sulfurs were added, and finally, a set of three calculations was performed with hydrogens added to the terminal sulfur atoms. The first of these had linear Co–S–H bonds, which preserve octahedral symmetry, but are unrealistic. The second had bonds bent at an angle of 113°, but arranged in such a way that D_{4h} symmetry was retained. Finally, the Co–S–H bonds were twisted, changing the S_b Co–S–H dihedral angles by 45° and destroying most of the remaining symmetry to that of the D_{2h} point group. Burdett and Miller also performed calculations on the first three of these clusters, with almost identical bond lengths, but did not present any results for the reduced symmetry clusters.

Table III. MS-Xα Parameters for Model Clusters

	l_{max}	α	sphere radius (a_0) $Co_8S_{14}^{12-}$	$Co_8S_6(SH)_8^{4-,5-,6-}$	$Co_8(SH)_6(SH)_8^{2+}$
int		0.71803			
out	5	0.71803	11.0348	10.8575	10.8575
Co	2	0.71018	2.2401	2.2399	2.2392
S_b	1	0.72475	2.2783	2.2783	2.1811
S_t	1	0.72475	2.6466	2.4148	2.4147
H_t	0	0.77725		1.01	1.01
H_b	0	0.77725			1.01

b. MS-Xα Calculations. A deficiency of EHT is that the Hamiltonian matrix elements are determined from empirical considerations that reflect mainly the connectivity of the atoms in the molecule. These values are independent of the total number of electrons so that effects due to changes in oxidation state are reflected only in a different occupation of the fixed orbitals; the orbital energy spectrum and eigenfunctions are independent of such changes. Similarly, effects on a large cluster due to the addition of ligands to outer atoms are not expected to be as well modeled with EHT if the connectivity of the central core is not significantly modified. By performing MS-Xα calculations, we are able to take the electron–electron interactions into account explicitly and effects due to the changes just mentioned will be more realistically described.

The nuclear coordinates and selected interatomic distances for the clusters are presented in Table II. All the clusters studied contain a skeletal Co_8S_{14} structure which, taken by itself, belongs to the O_h point group. The bond lengths of this structure were chosen to lie within the ranges given by the experimentally measured values for the two 4- anionic species. The effects of the phenyl groups are estimated by adding hydrogen atoms to the terminal sulfurs with a bond length equal to that of an organic thiol (see Table II). The dihedral angle for the thiol group was chosen so that D_{4h} symmetry is retained. The presence of additional symmetry allows the calculations to be performed more easily, and the particular dihedral angle used is expected to have a negligible effect on the core cluster electronic properties.[10,11] There are two ways the thiol group can be oriented to satisfy this criterion. One has the hydrogens attached to the four terminal sulfurs on the faces perpendicular to the C_4 axis pointing toward the axis; alternatively, the hydrogen atoms could point away from the axis. Since the second alternative results in less crowding of the hydrogen atoms, this geometry was selected. Hydrogen atoms were also attached to the bridging sulfurs to mimic the effects on the core structure of the intercluster connections in the bulk pentlandite. These S–H bonds were directed straight out from the center of the cluster and had a bond length equal to that of an organic thiol.

The MS-Xα calculations were performed using the programs developed by Cook and Case,[15] based on the program of K. H. Johnson and F. C. Smith, Jr. Detailed descriptions of the MS-Xα method are given elsewhere.[9] Here we discuss only certain aspects of the calculations that are specific to the present application. A number of parameters must be specified, and the values used are presented in Table III. A minimum basis set was used, i.e., the l_{max} values were chosen to reflect the shell structures of the isolated atoms: 2 for cobalt spheres (s,p,d shells), 1 for sulfur spheres (s,p shells), and 0 for hydrogen spheres (s shell). For the outer sphere to have components for all the irreducible representations of the O_h point group, the value of l_{max} here was set to 5. The α values used are the α_{HF} values of Schwarz[16] for the cobalt and sulfur atomic spheres. For the hydrogen atomic spheres, the spin-polarized value suggested by Slater[17] was used. The value of α assigned to the intersphere region and the outer sphere was determined by averaging the values for the atomic spheres, weighted by the number of valence electrons contributed by the atoms. For these calculations, all the orbitals up to and including Co 3p and S 2p are treated as core levels. This puts 284 electrons into cores and 168 electrons in the valence levels for all but the 5- and 6- anions, which contain 169 and 170 valence electrons. In performing MS-Xα calculations, the core orbitals are assumed to be confined to the atomic spheres, in which the potential is spherically averaged.[9] This allows these orbitals to be expressed as radial functions times spherical harmonics, and the radial functions are easily obtained

(12) Hoffmann, R. *J. Chem. Phys.* **1963**, *39*, 1397–1412.
(13) Burdett, J. K. *Molecular Shapes*; Wiley-Interscience: New York, 1980; p 28.
(14) Ammeter, J. H.; Bürgi, H.-B.; Thibeault, J. C.; Hoffmann, R. *J. Am. Chem. Soc.* **1978**, *100*, 3686–3692.
(15) Cook, M.; Case, D. A. *Quantum Chemistry Program Exchange* Bloomington, IN, *No. 465*.
(16) Schwarz, K. *Phys. Rev. B.* **1972**, *5*, 2466–2468.
(17) Slater, J. C. *Int. J. Quantum Chem.* **1973**, *S7*, 533–544.

through numerical integration of the one-dimensional differential equations. The determination of the core orbitals therefore comprises a very small part of the calculation and it costs little to include them explicitly in the self-consistent procedure.

The electrons were placed in orbitals in such a way that the lowest energy orbitals were occupied. For the spin-polarized calculations, such a criterion can lead to high-spin states since increasing the charge density of one spin has the effect of lowering the energies of the other orbitals with that spin relative to those of opposite spin orbitals.[18] The fact that low-spin states were observed in this study is therefore a reliable result and not an artifact of the MS-Xα technique. The calcualtions performed were spin-restricted except in the case of the $[Co_8S_{14}H_8]^{4-,5-,6-}$ clusters, for which spin-polarized calculations were also performed.

The atomic sphere radii were chosen by means of the Norman criterion.[19] Spheres were constructed around each nucleus, which contain the atomic number of electrons. To avoid excessive overlap, the radii were then all reduced by a constant factor. The factor used here was 0.85 and is consistent with other MS-Xα calculations.[18] It should be noted that the Norman criterion gives different sphere sizes as atoms are added to the cluster. In particular, when a hydrogen atom is attached to a sulfur, the added hydrogen atom contribution to the starting potential allows a smaller sphere about the sulfur atom to contain the atomic number of electrons. A consequence of this is that the sulfur atom sphere is substantially reduced in size, reflecting its reduced sphere of influence when it is bonded to more atoms. For the hydrogen atomic spheres, the Norman criterion results in a radius that is considered to be too large on the basis of calculated one-electron properties.[20,21] For these atoms, a sphere size of $1.01a_0$ has been found to yield more reasonable results.[20-23] Finally, the outer-sphere radius was chosen to be $0.20a_0$ smaller than a sphere tangent with the outermost atomic sphere. It is desirable to reduce the volume of the intersphere region in a MS calculation,[22] and this reduction is one way to accomplish this.

Because of the high charges on the clusters, Watson spheres[24] of canceling charge were placed at the outer-sphere radii to mimic the counterion environment. This has the effect of keeping the charge density of a negative ion from becoming too diffuse and that of a positive ion from becoming too compact. An adverse effect of the use of different Watson sphere charges or different atomic sphere sizes is that they tend to shift the valence orbital energies, making direct comparison of orbital energies for two different species impossible. However, the relative orderings and spacings are not greatly affected,[25] so that comparison of orbital energy orderings, level splittings, and the like, are meaningful.

To examine the effect of added electrons on the structure, the Hellmann-Feynman theorem[26] was used. According to this theorem, which is obeyed by the Xα Hamiltonian,[27] the force on nucleus i in a molecule is obtained from the equation

$$\mathbf{F}_i = -Z_i\left[\sum_{j\neq i}\frac{Z_j\mathbf{R}_{ij}}{R_{ij}^3} - \int\frac{(\mathbf{R}_i - \mathbf{r})}{|\mathbf{R}_i - \mathbf{r}|^3}\rho(\mathbf{r})d^3r\right]$$

where $\mathbf{R}_i$ is the position of nucleus i, $\mathbf{R}_{ij}$ is the vector from nucleus i to nucleus j, and $\rho(\mathbf{r})$ is the electronic density. In this study, the density is constructed from MS-Xα orbitals, and the integral over the electron density is easily evaluated by the charge partitioning technique of Case and Karplus.[28] In the calculations that follow, these forces are expressed in atomic units, where 1 au of force = 1 electron charge/bohr radius.

When the MS technique is used, certain approximations are introduced that make the Hellmann-Feynman theorem only approximately true. It is therefore not reliable for geometry optimization, as has been illustrated explicitly for the iron dimer.[29] However, it is expected to give a qualitative estimate of the effect of changes in the electronic density on the molecular structure; i.e., although a nucleus in a stable reference structure may have a nonzero Hellmann-Feynman force when calculated from the above equation, it is expected that the structure of the molecule would respond to a change in the force due to a change in the charge distribution of the molecule. In the present calculations, the density of the $[Co_8S_6(SH)_8]^{4-}$ cluster is affected by adding hydrogens or electrons. Comparison of the electronic contribution for different oxidation states is straightforward, but the addition of hydrogen atoms introduces an additional change in the internuclear forces. The hydrogen atoms are added to the cluster to mimic the extra coordination of the solid by their effect on the electronic density of the core. However, the S-H bond length is much smaller than the corresponding Co-S bond length of 2.36 Å in the mineral structure[30] so that it is not reasonable to include this internuclear contribution as representative of the interactions in the extended material. If the larger bond length were used for the placement of the additional hydrogen nuclei, their contribution to the internuclear forces would be significantly reduced. Further, since less than half of an electron remains on each of these hydrogens in these calculations, the electronic contributions to the Hellmann-Feynman force are due almost entirely to changes in the electronic density of the core structure. Therefore, comparison of only the second term in the above equation is presented in the following analysis.

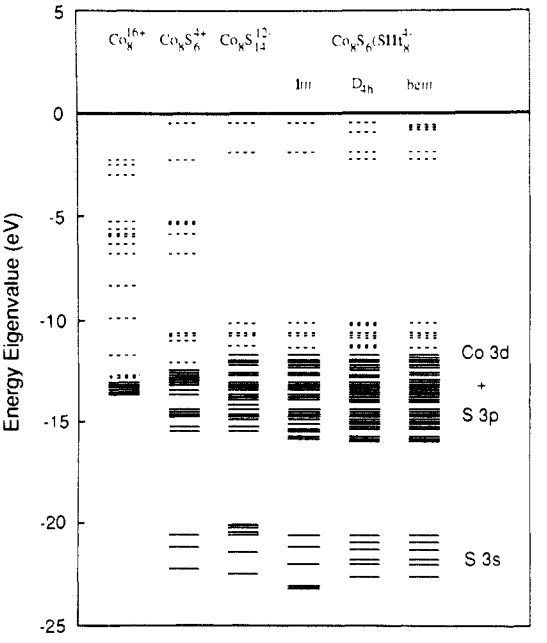

Figure 2. Valence orbital energy levels for various cobalt-sulfur clusters from extended Hückel theory calculations. Occupied levels are denoted by solid lines and virtual levels by dashed lines. The three $Co_8S_6(SH)_8^{4-}$ calculations correspond to different Co-S-H bond orientations: lin refers to a linear bond, D_{4h} refers to a bond bent such that D_{4h} symmetry is retained, and bent refers to bent bond twisted by 45° from the D_{4h} structure.

For the valence orbitals, the charge distributions were calculated in terms of the total charge in each of the partitioned regions used in the MS technique. To make analysis easier, the total charges are presented as percents of an electron and as sums for the atoms of a particular type. Thus, if each cobalt atom has 8% of an electron in a given orbital, the number reported for all the cobalt atoms is 8 times this, or 64%. A useful feature of these charge distributions is that bonding and nonbonding orbitals can be identified through the amount of intersphere charge. Bonding and antibonding orbitals should have a significant amount of electron charge between the atoms, while the opposite is expected for nonbonding orbitals. When this information is coupled with the particular types of spheres that have significant charge, the orbitals can be identified according to which atoms they bind. Previous MS-Xα studies[18] have used a similar technique, but have not included the information of the intersphere charge.

3. Results and Discussion

a. Extended Hückel Theory. Figure 2 presents the one-electron orbital energies obtained in the sequence of calculations. The graph indicates that there is little effect on the basic orbital energy spectrum due to the terminal sulfurs and hydrogens. The 3d orbitals of the cobalt atoms in the bare cubic cluster combine to

(18) Cook, M.; Karplus, M. *J. Chem. Phys.* **1985**, *83*, 6344-6366.
(19) Norman, J. G., Jr. *Mol. Phys.* **1976**, *31*, 1191-1198.
(20) Cook, M.; Karplus, M. *J. Chem. Phys.* **1980**, *72*, 7-19.
(21) Case, D. A.; Cook, M.; Karplus, M. *J. Chem. Phys.* **1980**, *73*, 3294-3313.
(22) Herman, F.; Williams, A. R.; Johnson, K. H. *J. Chem. Phys.* **1974**, *61*, 3508-3522.
(23) Case, D. A.; Karplus, M. *J. Am. Chem. Soc.* **1977**, *99*, 6182-6194.
(24) Watson, R. E. *Phys. Rev.* **1958**, *111*, 1108-1110.
(25) Kai, A. T.; Larsson, S. *Int. J. Quantum Chem.* **1978**, *13*, 367-374.
(26) Merzbacher, E. *Quantum Mechanics*; John Wiley & Sons, Inc.: New York, 1970; p 442.
(27) Slater, J. C. *Quantum Theory of Molecules and Solids*; Mc-Graw Hill Book Co.: New York, 1974; Vol. 4, pp 287-289.
(28) Case, D. A.; Karplus, M. *Chem. Phys. Lett.* **1976**, *39*, 33-38.
(29) Hoffman, G. G. Ph.D. Thesis, Harvard University, Cambridge, MA, 1987; pp 265-288.
(30) Rajamani, V.; Prewitt, C. J. *Can. Mineral.* **1975**, *13*, 75-78.

form a dense band of molecular orbitals near −13 eV and the introduction of the bridging sulfurs in $[Co_8S_6]^{4+}$ broadens the band by allowing interactions between the cobalt 3d and sulfur 3p orbitals. These interactions are strongest in the range −5 to −8 eV, where the cobalt orbitals that combine with the sulfur orbitals are significantly raised or lowered in energy. The sulfur 3s orbitals lie too low in energy (−20 to −23 eV) to combine with the cobalt orbitals and form a band of nonbonding orbitals of their own. The orbital energies in the frontier region, −10 to −15 eV, are in agreement with those of Burdett and Miller, as reported in their Figure 6.[8] The addition of the terminal sulfurs has almost no effect on the orbital spectrum, except that the remaining cobalt orbitals in the range −5 to −8 eV have combined with the sulfur orbitals, leading to strongly stabilized or destabilized molecular orbitals. Again, the frontier orbital energies agree with those presented by Burdett and Miller in their Figure 8.[8] The addition and reorientation of the hydrogen atoms causes almost no changes; the only visible effect is the lifting of certain degeneracies by the introduction of small splittings. The most important aspects of the orbital energy spectrum seem to be due to the interactions of the cobalt atoms and the bridging sulfur atoms.

An extensive EHT analysis of some of these clusters, in addition to the bulk Co_8S_8 and Co_9S_8 systems, is presented by Burdett and Miller.[8] They also found that the dominant factor contributing to the orbital spectrum was the Co–S_b interaction; that is, the metal-bridging sulfur interactions are maximized at the expense of metal–metal interactions. Orbitals that would be considered to be Co–S_b antibonding were not occupied even if they would contribute to the metal–metal bonding.

b. MS-Xα Calculations. $[Co_8S_{14}]^{12-}$. MS-Xα calculations were first performed on the ideal $[Co_8S_{14}]^{12-}$ cluster with octahedral symmetry (Figure 1). The 12− total charge was chosen to keep the system consistent with the 4− cluster. Because of the high symmetry, there are only three symmetry-distinct atoms (i.e., Co, S_b, and S_t). The valence orbital one-electron energies and charge distributions are given in Table IV. The orbital energy spectrum shows a structure similar to the EHT results. There are tight bands of essentially nonbonding sulfur 3s orbitals at −18 eV for the bridging sulfurs and at −14.5 eV for the terminal sulfurs. The next band of orbitals from −9.5 to −8.5 eV are composed of combinations of cobalt 3d and bridging sulfur 3p atomic orbitals. Due to the significant amount of intersphere charge in this band, these can be interpreted as framework bonding orbitals. At about −6.5 eV, a band of Co–S_t orbitals is found that are principally combinations of sulfur 3p and cobalt 3d orbitals. Starting at about −6 eV, a dense band of orbitals is found that are combinations of Co–S_t orbitals as well as cobalt nonbonding orbitals. Overall, the most noticeable features of the electronic structure are the isolated sulfur 3s bands and the low-energy framework bonding orbitals in the range −9.5 to −8.5 eV.

It is useful to correlate these results with a simple molecular orbital (MO) picture. The calculations performed indicate that the atomic orbitals up to the sulfur 3s and up to the cobalt 3p orbitals are localized core orbitals. The important interactions are therefore between the cobalt 4s, 3d orbitals and the sulfur 3p orbitals. These sets of orbitals can be decomposed into symmetry-adapted orbitals for the O_h point group as follows.

AO	no. of orbitals	decomposition
Co 4s	8	$a_{1g} + a_{2u} + t_{1u} + t_{2g}$
Co 3d	40	$a_{1g} + a_{2u} + 2e_g + 2e_u + 2t_{1g} + 3t_{1u} + 3t_{2g} + 2t_{2u}$
S_b 3p	18	$a_{1g} + e_g + t_{1g} + 2t_{1u} + t_{2g} + t_{2u}$
S_t 3p	24	$a_{1g} + a_{2u} + e_g + e_u + t_{1g} + 2t_{1u} + 2t_{2g} + t_{2u}$

Assuming interactions only between nearest neighbors, these orbitals combine to form sets of 18 bonding and 18 antibonding Co–S_b orbitals, sets of 24 bonding and 24 antibonding Co–S_t orbitals, and a set of six nonbonding Co orbitals (a_{2u}, t_{2g}, e_u).

The interactions of the cobalts with the bridging sulfurs seem to be stronger than with the terminal sulfurs, since the bonding orbitals with the bridging sulfurs are lower in energy. That the band at −9.5 to −8.5 eV is the set of bonding combinations is supported by contour plots of the orbitals. Due to the stronger interactions, the set of antibonding Co–S_b orbitals should be higher in energy than all the Co–S_t orbitals, bonding or antibonding. Based on symmetry assignments and the population analysis in Table IV, the Co–S_t bonding orbitals are contained in a band from the $4a_{1g}$ (−6.56 eV) to the $6t_{1u}$ (−5.18 eV) orbitals. At first glance, the $3e_g$ (−5.72 eV) orbital may be thought to be a nonbonding cobalt orbital. However, it is more reasonable to assign this to a weakly interacting bonding combination that is predominantly cobalt in character, since the associated $4e_g$ (−5.07 eV) orbital can be assigned to the weakly antibonding combination that is predominantly sulfur in character. The nonbonding cobalt orbitals are comprised of a_{2u}, t_{2g}, and e_u combinations. The $2e_u$ (−5.12 eV) and $5t_{2g}$ (−4.68 eV) orbitals can be assigned to this set, but a nonbonding a_{2u} orbital cannot be found. Since the simple picture of only nearest-neighbor atoms interacting is not exact and the

Table IV. One-Electron Energies and Charge Distributions for $Co_8S_{14}^{12-}$ [a]

orbital	ϵ (eV)	Co	S_b	S_t	out	int	
$9t_{1u}$*	−2.71	56	21	10	3	10	Co–S
$4t_{1g}$*	−2.98	66	21	5		8	antibonding
$7t_{2g}$*	−3.03	57	7	23	3	10	(unoccupied)
$5e_g$*	−3.34	61	15	7	2	15	
$8t_{1u}$	−3.60	64	5	17	2	12	
$3a_{2u}$	−3.67	68		20	2	10	
$4t_{2u}$	−3.81	43	7	32	2	16	
$3e_u$	−3.91	50		36	2	12	
$3t_{1g}$	−3.98	55		31	1	13	
$6t_{2g}$	−4.18	40		41	2	17	
$7t_{1u}$	−4.27	63	2	22	1	12	
$5a_{1g}$	−4.44	49	3	26	2	20	
$2e_u$	−4.68	95		1		4	mix
$4e_g$	−5.07	10	6	55	2	27	
$5t_{2g}$	−5.12	92	1	1		6	
$6t_{1u}$	−5.18	28	7	45	1	19	
$3t_{2u}$	−5.38	62	1	18	1	18	
$1e_u$	−5.39	48		37	1	14	
$2t_{1g}$	−5.45	46		37	1	16	
$3e_g$	−5.72	87	3	3		7	
$4t_{2g}$	−5.75	52		29	1	18	
$2t_{2u}$	−5.99	67		18	1	14	
$2a_{2u}$	−6.38	40		51	3	6	
$3t_{2g}$	−6.45	43		48	3	6	Co–S_t
$5t_{1u}$	−6.50	44	1	46	3	6	
$4a_{1g}$	−6.56	44	5	41	2	8	
$1t_{2u}$	−8.52	24	60			16	
$2e_g$	−8.55	30	51	1		18	
$4t_{1u}$	−8.61	27	54	1		18	
$1t_{1g}$	−8.74	32	54			14	Co–S_b
$3a_{1g}$	−9.22	17	56	1		26	
$2t_{2g}$	−9.33	23	54	1		22	
$3t_{1u}$	−9.58	28	51	1		20	
$1a_{2u}$	−14.64	3		88	1	8	
$2a_{1g}$	−14.65	3		88	1	8	S_t 3s
$2t_{1u}$	−14.66	3		88	1	8	
$1t_{2g}$	−14.66	3		88	1	8	
$1e_g$	−18.24	7	83			10	
$1t_{1u}$	−18.41	8	81			11	S_b 3s
$1a_{1g}$	−18.77	9	77			14	
Co 3p	−60.78						
Co 3s	−94.95						
S_t 2p	−153.78						
S_b 2p	−156.24						
S_t 2s	−206.84						
S_b 2s	−209.36						core
Co 2p	−762.65						
Co 2s	−877.40						
S_t 1s	−2393.00						
S_b 1s	−2394.85						
Co 1s	−7506.48						

[a] For each orbital, this table presents (i) the orbital symmetry, (ii) the orbital energy (in eV), and (iii) the charge distribution as the percentages of the orbital that is in the specified atomic spheres, outer sphere (out), and the intersphere region (int). The final column designates the types of orbitals in each band obtained from an interpretation of the charge distributions. Unoccupied orbitals are asterisked.

Table V. One-Electron Energies and Charge Distributions for Spin-Restricted $Co_8S_6(SH)_8^{4-a}$

orbital	ϵ (eV)	Co	S_b	S_t	H	out	int	
$9a_{2u}$*	−5.16	56	24	10		1	9	
$13e_u$*	−5.21	58	24	9		1	8	
$11e_g$*	−5.47	66	22	4			8	
$4a_{2g}$*	−5.48	66	22	4			8	unoccupied
$7b_{1g}$*	−5.56	57	8	24		2	9	
$10e_g$*	−5.69	61	8	20		2	9	
$5b_{2g}$*	−5.76	61	17	9		1	12	
$10a_{1g}$*	−5.86	64	22	2			12	
$12e_u$	−6.08	62	5	20		2	11	
$6b_{2u}$	−6.21	65		22		2	11	
$4b_{1u}$	−6.31	43	8	33		1	15	
$8a_{2u}$	−6.35	70	6	12		2	10	
$3a_{1u}$	−6.47	48		38		1	13	
$3a_{2g}$	−6.53	53		34			13	
$11e_u$	−6.55	52	7	26		1	14	
$9e_g$	−6.67	42		41		1	16	
$7a_{2u}$	−6.91	79	5	9			7	
$9a_{1g}$	−6.92	49	3	27		1	20	
$5b_{2u}$	−7.07	93		2	1		4	
$10e_u$	−7.10	81	6	3	1		9	
$8e_g$	−7.13	85	1	7	1		6	
$2a_{1u}$	−7.24	95		1			4	
$4b_{2u}$	−7.28	96		1			3	
$4b_{2g}$	−7.46	9	6	56		1	28	
$6b_{1g}$	−7.53	91		2	1		6	mix
$7e_g$	−7.66	93	1	1			5	
$9e_u$	−7.68	35	5	39		1	20	
$5b_{1g}$	−7.72	91	2	1			6	
$3b_{1u}$	−7.79	55	2	23			20	
$1a_{1u}$	−7.87	50		34		1	15	
$2a_{2g}$	−7.93	48		35			17	
$6e_g$	−8.11	50	1	31		1	17	
$8a_{1g}$	−8.19	90	1	1			8	
$8e_u$	−8.23	81		9		1	9	
$3b_{2g}$	−8.24	87	3	2			8	
$2b_{1u}$	−8.46	74		14			12	
$3b_{2u}$	−8.55	36		48	1	2	13	
$6a_{2u}$	−8.55	36	5	44	1	1	13	
$4b_{1g}$	−8.61	35		48	1	2	14	
$7a_{1g}$	−8.67	39	6	39	1	1	14	
$5e_g$	−8.68	42		42	1	1	14	
$7e_u$	−8.75	44		40		2	14	
$6a_{1g}$	−10.63	26	42	13	4	1	14	
$5a_{2u}$	−10.73	30	47	5	1	1	16	
$6e_u$	−10.74	27	49	8	2	1	13	
$5e_u$	−10.85	20	47	11	3	1	18	
$1b_{1u}$	−10.91	26	60				14	
$4e_g$	−10.91	26	26	28	8	1	11	
$2b_{2g}$	−10.91	31	51	1			17	
$2b_{2u}$	−11.05	10		59	16	2	13	
$5a_{1g}$	−11.05	13	29	29	8	1	20	
$3b_{1g}$	−11.08	12	4	54	15	1	14	Co–S
$4a_{2u}$	−11.08	13	7	51	14	2	13	
$3e_g$	−11.11	25	34	21	6	1	13	
$1a_{2g}$	−11.15	34	53				13	
$4e_u$	−11.16	22	22	32	9	1	14	
$4a_{1g}$	−11.56	20	38	17	4	1	20	
$2e_g$	−11.68	20	46	10	3		21	
$2b_{1g}$	−11.70	23	51	4	1	1	20	
$3e_u$	−11.92	27	46	6	2		19	
$3a_{2u}$	−11.95	29	48	3	1		19	
$2a_{2u}$	−18.53	2		81	7	2	8	
$1b_{2u}$	−18.54	2		82	7	2	7	
$2e_u$	−18.54	2		81	7	2	8	S_t
$3a_{1g}$	−18.54	2	1	81	7	1	8	
$1e_g$	−18.54	2		82	7	1	8	
$1b_{1g}$	−18.56	2		81	7	2	8	
$2a_{1g}$	−20.43	8	82				10	
$1a_{2u}$	−20.53	8	81				11	
$1b_{2g}$	−20.66	8	83				9	S_b
$1e_u$	−20.83	8	81				11	
$1a_{1g}$	−21.09	9	78				13	
Co 3p	−63.35							
Co 3s	−97.50							
S_t 2p	−156.62							
S_b 2p	−158.52							
	−158.68							
S_t 2s	−209.69							
S_b 2s	−211.64							core
	−211.80							
Co 2p	−765.13							
Co 2s	−879.87							
S_t 1s	−2395.66							
S_b 1s	−2397.17							
	−2397.26							
Co 1s	−7509.00							

[a] See Table IV.

bonding and nonbonding orbitals of a given symmetry can form linear combinations, this MO description serves only as a rough guide. The antibonding Co–S_t combinations form a band that slightly overlaps the band of bonding combinations, ranging from the $3t_{2u}$ (−5.38 eV) to the $7t_{2g}$* (−3.03 eV) orbitals (an asterisk indicates that the orbital is unoccupied). Based on the population analysis, the lowest antibonding Co–S_b orbital is the $5e_g$* (−3.34 eV) level. A problem with this analysis is that it leaves the $4t_{2u}$ (−3.81 eV) level unassigned. Arguing solely on the basis of the decomposition of the AOs presented earlier, this may be interpreted as an antibonding Co–S_b orbital. However, it has very little bridging sulfur character and would be expected to be only weakly antibonding, if at all. In summary, the gross features of the orbital spectrum (i.e., the low-energy framework bonding orbitals, the band of Co–S_t bonding and antibonding orbitals, and the unoccupied antibonding Co–S_b orbitals) are consistent with a simple MO analysis. However, the assumptions of this analysis are rather simple and are insufficient to explain some specific details.

$[Co_8S_6(SH)_8]^{4-}$. To study the effect of ligands on the terminal sulfurs on the orbital energy spectrum, protons were added to the cluster. According to the EHT calculations, the results should be very similar. The one-electron energies and charge distributions are given in Table V. The results are similar to the previous calculation: however, there are certain distinct differences due to the presence of the hydrogens. As mentioned (see section 2), the absolute values of the energies cannot be compared with the previous calculations, due to the overall shift expected from the different charge on the Watson sphere and the different sphere sizes. However, a correlation can be made in the relative energies.

Two tight bands at −21 and −18.5 eV are observed for the nonbonding sulfur 3s orbitals. The terminal sulfur levels at −18.5 eV include small contributions from the hydrogen atoms. A dense band of orbitals at −10 to −12 eV contain significant contributions from the cobalt and sulfur atoms. Instead of having two discrete bands, one for the bridging sulfurs and one for the terminal sulfurs, the two types of orbitals are mixed together. In addition, near −11 eV, there are several orbitals with significant contributions from the hydrogen atoms as well. The rest of the orbitals form a dense band of mixed types from −9 to −5 eV. The orbital energies are compared with those for the cluster without hydrogens in Figure 3. The only significant difference is the effect on the orbitals with terminal sulfur contributions. The hydrogens seem to stabilize these orbitals relative to the Co–S_b orbitals and the two types of bonding orbitals are able to mix. The main features, though, are still the same; i.e., there are low-energy bands for the nonbonding sulfur 3s orbitals, a low-energy band for the framework bonding orbitals, and a dense band up to the virtual orbitals. This is just what is observed in the EHT calculations (see Figure 2), though the stabilizing effect of mixing is not observed.

Recalling the MO theory arguments presented in the previous calculation, the stabilization of the Co–S_t bonding orbitals implies a destabilization of the Co–S_t antibonding orbitals. It may be expected, then, that some of the Co–S_b antibonding orbitals could now be occupied. However, correlation of the orbitals based on symmetry arguments shows that none of the unoccupied orbitals of $[Co_8S_{14}]^{12-}$ become occupied upon the addition of hydrogens.

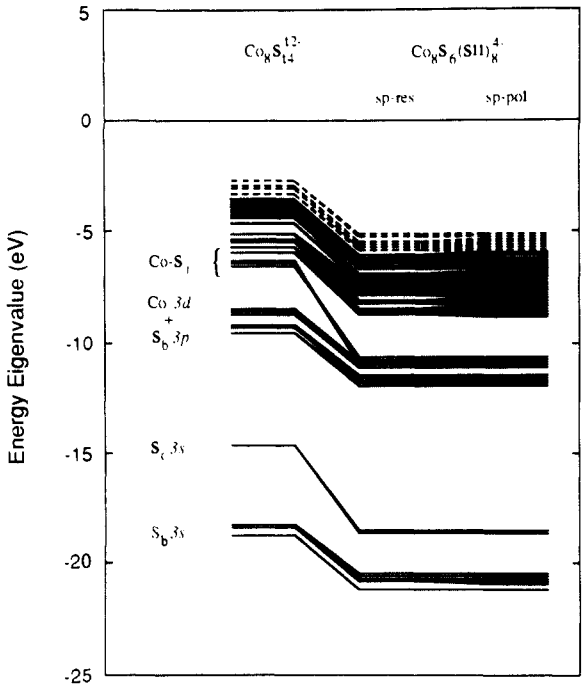

Figure 3. Correlation diagram for the valence orbitals for MS-Xα calculations on several of the clusters.

Further, the bridging sulfur character of all the occupied orbitals remains small, aside from the bonding orbital combinations, which are low in energy.

Spin-polarized calculations were also performed on this cluster. Assuming spin pairing in all the lower energy orbitals, the only partially filled orbital is the half-filled $12e_u$ level and there are two possible spin states associated with this configuration. The spin-paired case, corresponding to the spin-restricted calculation just described, and the spin-polarized case, with the two electrons having the same spin, were studied. The orbital energy levels are included in Figure 3. Aside from some small splittings, the spin-restricted and spin-polarized energy levels for $[Co_8S_6(SH)_8]^{4-}$ are essentially identical. The spin-restricted orbital levels are split in the spin-polarized calculation by energies ranging from −0.01 to 0.2 eV and the total statistical energies differ by only 0.07 eV in favor of the spin-polarized configuration. With such a small difference, there is little reason to conclude that the triplet state is more stable. The singlet state deduced by Christou et al. is therefore consistent with these results.

In their calculations on $[Co_8S_6(SH)_8]^{4-}$, Burdett and Miller forced octahedral symmetry and observed a triply degenerate HOMO corresponding to the t_{1u} irreducible representation. Because there were four electrons in this orbital, they suggested that one of the electrons could occupy a higher energy t_{2g} orbital in order to relieve the spin-pairing energy. A t_{1u} HOMO is also found in the MS-Xα calculation for octahedral $[Co_8S_{14}]^{12-}$, but the addition of hydrogens with bent bonds reduces the symmetry and splits this level into a lower energy $8a_{2u}$ level and a half-filled $12e_u$ HOMO level. The spin-polarized calculation just described has the effect of relieving the spin-pairing energy within the $12e_u$ level. Since this has almost no effect on the total energy, the effect suggested by Burdett and Miller is not expected to occur.

A final consideration regarding this cluster involves the possibility of antiferromagnetic coupling among the cobalt atoms. Because of the even number of these atoms, a cube of spin $-^3/_2$ cobalt atoms could still result in a low-spin ground state, although the electronic spin density could be significantly different from the symmetry-restricted results obtained above. Such a possibility is generally taken into account through the application of broken symmetry calculations, where the cobalt atoms are no longer considered to be symmetry equivalent, coupled with spin-projection techniques.[31,32] This results in a reduction in the symmetry of the compound and a consequent increase in the computational effort. Nevertheless, in some clusters containing iron atoms, broken symmetry calculations[10,32] have produced significantly lower ground-state energies than symmetry-restricted calculations. A corresponding result has been obtained for iron–molybdenum clusters.[18]

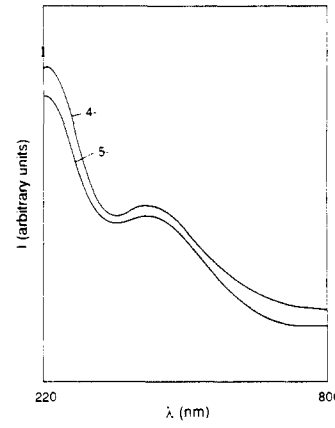

Figure 4. Comparison of calculated absorption spectra for the $Co_8S_6(SH)_8^{4-,5-}$ clusters. These qualitative results are equal-weight Gaussian peaks of symmetry-allowed excitation energies from occupied to virtual MS-Xα orbitals.

Calculations were performed in which alternating cobalt atoms were treated as if they were symmetry distinct, reducing the symmetry of the cluster to the D_{2d} point group. The ground state of this lower symmetry cluster was found to be negligibly different from the D_{4h} state found above. Antiferromagnetic coupling is therefore not expected to play a role in the bonding of these clusters.

$[Co_8S_6(SH)_8]^{5-}$. To treat the $[Co_8S_6(SH)_8]^{5-}$ system, a choice must be made as to where to put the extra electron. In both the singlet- (spin-restricted) and triplet- (spin-polarized) state calculations on $[Co_8S_6(SH)_8]^{4-}$, the highest occupied molecular orbital is the half-filled $12e_u$ level. The calculations yield energies that differ by a negligible amount, meaning that the exchange energy, which would favor the triplet state, plays a minor role in this structure. For this reason, it would be expected that an added electron would most likely go into the lower energy $12e_u$ level, leading to a spin-doublet state, as opposed to occupying the higher energy $10a_{1g}$* level (see Table V) to yield a quintet state. This is consistent with the observation made by Christou et al. that $[Co_8S_6(SPh)_8]^{5-}$ has a $S = {}^1/_2$ ground state. Because the $12e_u$ orbital has predominantly cobalt and terminal sulfur atom character, putting the extra electron in this level would not be expected to change the orbital energy level spectrum to any appreciable degree since the effect of the terminal sulfurs has been found in general to be small (see above).

Spin-polarized MS-Xα calculations were performed on the $[Co_8S_6(SH)_8]^{5-}$ cluster using the same molecular geometry and MS-Xα parameters as for the 4- cluster. The state in which all the lowest energy orbitals are occupied is precisely the doublet predicted above. The orbital spectra for the two oxidation states are nearly identical, supporting the observed similarity in the absorption spectra for the 4- and 5- clusters.[5] Calculated absorption spectra are shown in Figure 4. They were generated by determining the symmetry-allowed excitations in the dipole approximation from the occupied to virtual MS-Xα orbitals and then combining equal Gaussians centered at these energies. Because of the crude approximations made, these plots are of qualitative use only. However, the similarity in the two spectra is evident and there is a rough agreement with the experimental results.

Evaluation of the Hellmann–Feynman force on the cobalt atoms indicated a difference of only 0.04 au for the two oxidation states, the 5- structure having the larger inward force. The similarity

(31) Noodleman, L. *J. Chem. Phys.* **1981**, *74*, 5737–5743.

(32) Noodleman, L.; Baerends, E. J. *J. Am. Chem. Soc.* **1984**, *106*, 2316–2327.

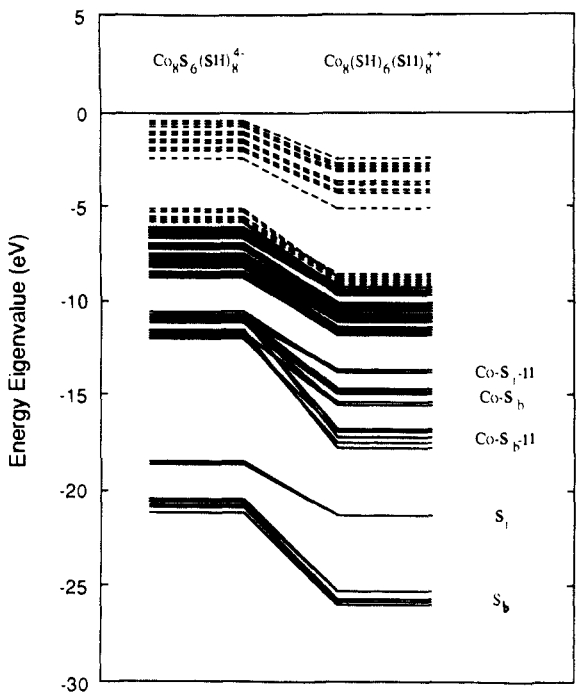

Figure 5. Correlation diagram illustrating the effect of adding hydrogens to the bridging sulfurs. Some higher energy levels not present in Figure 3 have been added here.

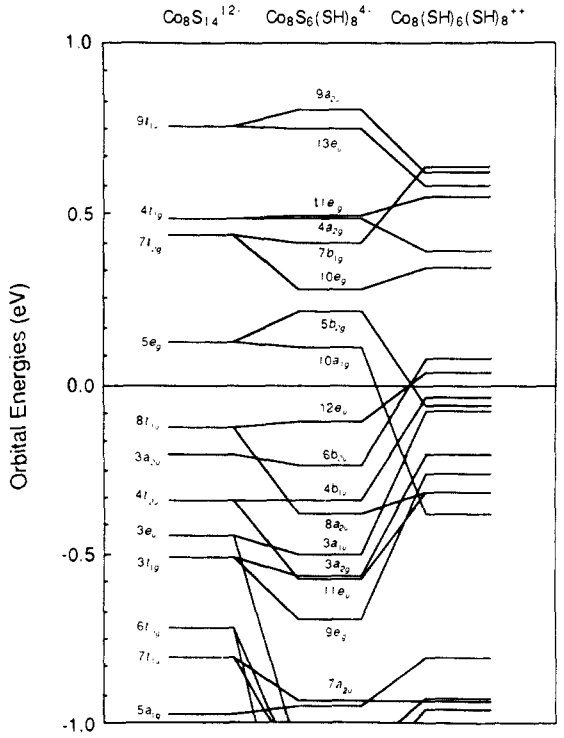

Figure 6. Expanded view of frontier orbital energies for the series of clusters $Co_8S_{14}^{12-}$, $Co_8S_6(SH)_8^{4-}$, and $Co_8(SH)_6(SH)_8^{2+}$. The MS-Xα orbital energies are shifted so that zero is halfway between the HOMO and LUMO of each set. All positive energy orbitals are unoccupied and all negative energy orbitals are occupied.

in the sizes of the structures of the $[Co_8S_6(SPh)_8]^{4-,5-}$ clusters is therefore consistent with these calculations, although the prediction that the 5- structure is slightly smaller is at odds with experiment.

Pentlandite Models. Two types of calculations were made to extrapolate from the clusters to cobalt pentlandite. One of these is the anion $[Co_8S_6(SH)_8]^{6-}$, which has the same formal charge on the cobalt atoms as bulk Co_9S_8, and the other is $[Co_8(SH)_6(SH)_8]^{2+}$, which has the extra interactions that arise from placing the core in the solid.

To extrapolate the results of the 4- and 5- cluster calculations to the 6- anion, it is necessary to determine the orbital occupied by the extra electron. One possibility is that the extra electron occupies the last $12e_u$ orbital leading to a closed-shell singlet ground state. However, the exchange energy gained in occupying the $10a_{1g}$* level may be more favorable here than in the 4- structure, even though this virtual level is observed to be a Co-S_b-type orbital and is of antibonding character. MS-Xα calculations for the two configurations indicate that the singlet state is more stable by 0.014 Ry (0.2 eV). The orbital eigenvalue spectrum is almost identical with those of the 4- and 5- species. It is therefore predicted that the $[Co_8S_6(SPh)_8]^{6-}$ cluster would have a spin singlet ground state and would have a UV-vis absorption spectrum nearly identical with the 4- and 5- clusters. The Hellmann-Feynman force for the 6- cluster was calculated to be 0.3 au greater, pointing inward, than the other oxidation states, indicating that this cluster would tend to be smaller in size, in accord with the crystal results.

Another possible model for cobalt pentlandite is the $[Co_8(SH)_6(SH)_8]^{2+}$ cluster. The substantially reduced size of the core in pentlandite could be due to the additional ligand bonding in the mineral. Since the previous calculations imply that the effect of the terminal sulfurs on the orbitals binding the cluster is small, the most probable source is the extra bonding to the bridging sulfurs by cobalt atoms. The intercluster cobalt atoms would be expected to have a formal positive charge due to their low electronegativity relative to the sulfur atoms, so that the effect of these ligands may be simulated in a MS-Xα calculation by introducing protons at the corresponding positions. We examine the relative ordering of the Co-S_b orbitals in the eigenvalue spectrum and compare the Hellmann-Feynman force on a cobalt atom in this cluster with that in the absence of hydrogens.

The one-electron energies and charge distributions are presented in Table VI. The overall scheme is similar to that from the other calculations, but there are some differences. There are contributions from the new hydrogen atoms to the nonbonding S_b 3s orbitals at about -25 eV, and there is a band of framework bonding Co-S_b orbitals at -17 eV that also has significant contributions from these hydrogen atoms. The rest of the framework bonding orbitals form a band of their own at -14 to -15 eV and contain no contributions from these hydrogens. The Co-S_t-H orbitals form a higher energy band at about -13.5 eV and there is a dense band of orbitals from -12 eV up to the virtual orbitals at about -9 eV. When hydrogen atoms were added to the terminal sulfurs in forming $[Co_8S_6(SH)_8]^{4-}$, the Co-S_t orbitals were lowered in energy and mixed with the Co-S_b orbitals, which were distinct in the $[Co_8S_{14}]^{12-}$ cluster. Adding hydrogens to the bridging sulfurs seems to have stabilized the Co-S_b bonding orbitals so that this mixing is no longer observed. The Co-S band is therefore split into three separate bands, as can be seen clearly in Figure 5. There is, in addition, a general downward shift in the eigenvalues due to the different sphere sizes and the different Watson sphere charge, which should not be interpreted as a physical effect.

With such a significant effect on the Co-S_b framework bonding orbitals, it is likely that the addition of the hydrogen atoms would have a significant effect on the size of the Co_8S_6 core; i.e., the stabilization of the framework bonding orbitals relative to the rest implies stronger binding in the core. Neglecting the effect due to the hydrogen nuclei (see section 2), the Hellmann-Feynman force on a cobalt atom of $[Co_8(SH)_6(SH)_8]^{2+}$ was 1.2 au greater, pointing toward the center of the cluster, than the value for the $[Co_8S_6(SH)_8]^{4-}$ structure. This indicates that the extra coordination to the bridging sulfurs would cause the cluster to shrink. This effect is about 4 times that calculated due to the oxidation state change in $[Co_8S_6(SH)_8]^{6-}$ and suggests that the significantly smaller size of this structure in the pentlandite is due to extra bonding involving the crystal lattice.

In support of this, an important change is observed in the frontier orbitals. Figure 6 presents an expanded view of the frontier orbitals for the series $[Co_8S_{14}]^{12-}$, $[Co_8S_6(SH)_8]^{4-}$ (spin-restricted), and $[Co_8(SH)_6(SH)_8]^{2+}$. To make the comparison easier, all the energies are shifted so that zero energy corresponds to the midpoint between the HOMO and LUMO of

Table VI. One-Electron Energies and Charge Distributions for $Co_8(SH)_6(SH)_8^{2+}$ [a]

orbital	ϵ (eV)	Co	S_b	S_t	H_t	H_b	out	int	
$7b_{1g}$*	-8.70	53	6	29			2	10	
$9a_{2u}$*	-8.71	53	15	21		1	1	9	
$13e_u$*	-8.75	54	15	19			1	11	
$11e_g$*	-8.78	54	7	28			1	10	unoccupied
$4a_{2g}$*	-8.95	64	17	11				8	
$10e_g$*	-8.99	73	18	2				7	
$6b_{2u}$*	-9.26	58		28			1	13	
$12e_u$*	-9.30	50	3	32		1	1	13	
$4b_{1u}$	-9.37	32	5	46			1	16	
$5b_{2g}$	-9.39	44	4	35		1	1	15	
$3a_{1u}$	-9.41	33		51			1	15	
$3a_{2g}$	-9.54	46	1	39				14	
$9e_g$	-9.60	30		51			1	18	
$11e_u$	-9.65	52	6	28			1	13	
$8a_{2u}$	-9.65	74	5	11			1	9	
$10a_{1g}$	-9.71	56	4	23		1	1	15	
$9a_{1g}$	-10.15	60	3	18		1	1	17	
$5b_{2u}$	-10.26	91		4	1			4	
$7a_{2u}$	-10.26	79	2	11	1	1		6	
$8e_g$	-10.30	83	1	9	1			6	
$10e_u$	-10.39	76	5	7	1			11	
$2a_{1u}$	-10.47	95		1				4	
$4b_{2u}$	-10.51	96		1				3	
$4b_{2g}$	-10.64	44	3	31		1	1	21	
$6b_{1g}$	-10.72	89		3	1			7	mix
$3b_{1u}$	-10.86	60	3	19				18	
$7e_g$	-10.90	91	1	2				6	
$1a_{1u}$	-10.92	66		22				12	
$9e_u$	-10.92	61	2	22		1		14	
$2a_{2g}$	-10.97	62		24				14	
$5b_{1g}$	-10.97	91	1	2				6	
$6e_g$	-11.16	62	1	23			1	13	
$8e_u$	-11.38	73		16	1			10	
$8a_{1g}$	-11.46	86		4	1			9	
$3b_{2u}$	-11.49	43		43	1		1	12	
$4b_{1g}$	-11.54	40		44	1		1	14	
$3b_{2g}$	-11.59	87		4				9	
$2b_{1u}$	-11.63	84		7				9	
$5e_g$	-11.68	52		35	1		1	12	
$6a_{2u}$	-11.68	48	1	36	1	1	1	12	
$7e_u$	-11.77	60		27			1	12	
$7a_{1g}$	-11.88	53	1	30	1	1	1	13	
$2b_{2u}$	-13.66	13		58	15		2	12	
$5a_{2u}$	-13.67	15		56	15		3	11	
$4e_g$	-13.68	16	1	56	15		1	11	Co–S_t–H
$6e_u$	-13.71	17	1	55	14		2	11	
$3b_{1g}$	-13.74	15		56	15		1	13	
$6a_{1g}$	-13.77	16	1	55	14		1	13	
$5e_u$	-14.17	22	60	1				17	
$3e_g$	-14.79	29	55	1				15	
$1b_{1u}$	-14.82	21	62					17	
$1a_{2g}$	-14.99	28	57					15	Co–S_b
$2e_g$	-15.38	21	56	1				22	
$2b_{1g}$	-15.48	21	57	1				21	
$4e_u$	-15.49	28	52	1				19	
$4a_{2u}$	-15.59	28	53	1				18	
$5a_{1g}$	-16.85	15	56			14		15	
$3a_{2u}$	-16.99	14	55			13		18	
$2b_{2g}$	-17.23	14	57			14		15	Co–S_b–H
$3e_u$	-17.46	13	56			14		17	
$4a_{1g}$	-17.76	11	55			14		20	
$2a_{2u}$	-21.30	2		83	6		2	7	
$1b_{2u}$	-21.31	2		83	6		1	8	
$2e_u$	-21.31	2		82	6		2	8	S_t–H
$1e_g$	-21.32	2		83	6		1	8	
$3a_{1g}$	-21.33	2		82	6		2	8	
$1b_{1g}$	-21.33	2		82	6		2	8	
$2a_{1g}$	-25.25	6	79			4		11	
$1a_{2u}$	-25.28	6	78			4		12	
$1b_{2g}$	-25.67	5	80			4		11	S_b–H
$1e_u$	-25.77	6	79			4		11	
$1a_{1g}$	-25.92	6	77			4		13	
Co 3p	-66.51								
Co 3s	-100.63								
S_t 2p	-160.13								
S_b 2p	-162.32								
	-162.77								
S_t 2s	-213.19								
S_b 2s	-215.49								
	-215.94								core
Co 2p	-768.07								
Co 2s	-882.80								
S_t 1s	-2399.31								
S_b 1s	-2400.56								
	-2400.97								
Co 1s	-7512.05								

[a] See Table IV.

each set. There is no change in orbital occupations when hydrogens are added to the terminal sulfurs, but when hydrogens are added to the bridging sulfurs, the $10a_{1g}$ and $5b_{2g}$ orbitals, which drop significantly in energy, become occupied, while the $12e_u$ and $6b_{2u}$ orbitals become unoccupied. The newly occupied orbitals are correlated with the $5e_g$ level of the octahedral complex. The stabilization of an e_g level upon the introduction of extra coordination with the bridging sulfurs was also observed by Burdett and Miller.[8] This effect was attributed to an increase in the metal–metal bonding interactions in these orbitals. The significant reduction in the bridging sulfur contributions to these orbitals implies an additional reduction in the Co–S_b antibonding character of these orbitals, stabilizing them and allowing them to be occupied. These two newly occupied orbitals make a significant contribution to the increase in Hellmann–Feynman force on the cobalt atoms (0.8 au), but this is offset by the nearly equal decrease in the force due to the loss of the orbitals they replace. The increase in the Hellmann–Feynman force is therefore a rather subtle effect. The change cannot be attributed to any one or a few orbitals, but seems to be a combined effect.

4. Conclusions

MS–Xα calculations have been performed on a series of clusters, each containing the octahedral Co_8S_{14} core. There is a general structure to the orbital spectra of these species that, for the most part, is in agreement with the EHT results. The sulfur 3s orbitals lie too low in energy to mix effectively with the cobalt valence orbitals, so that all the bonding between these atoms occurs with the cobalt 4s, 3d and sulfur 3p orbitals. This leads to a tight band of nonbonding sulfur 3s orbitals at low energy, a separate band of bonding Co–S orbitals, slightly higher in energy, a broad band containing a mixture of different types of orbitals (nonbonding cobalt and Co–S_t bonding and antibonding orbitals), and then a set of unoccupied orbitals that are almost all antibonding Co–S_b orbitals. The antibonding Co–S_b orbitals are always unoccupied, an observation that agrees with a central result of Burdett and Miller,[8] who concluded that the stability of such structures is influenced by optimization of the Co–S_b interactions.

A number of details are brought out in the MS–Xα calculations that are not observed in the EHT results. In particular, the separate band of lower energy Co–S bonding orbitals is not observed in the EHT calculations. The structure of this band is also observed to change in the MS–Xα calculations as hydrogen atom ligands are added. The general rule is that the addition of a hydrogen atom to a sulfur leads to a stabilization of the interaction of that sulfur with the cobalts. For the $[Co_8S_{14}]^{12-}$ cluster, with no hydrogens, this band is composed entirely of framework bonding Co–S_b orbitals. Adding hydrogens to the terminal sulfurs leads to a stabilization of some of the Co–S_t orbitals that then mix with the framework bonding orbitals. Adding hydrogens then to the bridging sulfurs stabilizes the framework bonding orbitals so that this band is split up. In all cases, the framework bonding orbitals are in this band, well below the HOMO–LUMO region.

The $[Co_8S_6(SH)_8]^{4-,5-}$ clusters are models for the $[Co_8S_6(SPh)_8]^{4-,5-}$ clusters synthesized by Christou et al.[5] The ground state of the 4– structure has a half-filled $12e_u$ HOMO, and al-

though the triplet-state configuration has a lower MS-Xα energy, the difference between it and the singlet state is too small to be confident of this ordering. The observed singlet ground state is therefore not inconsistent with the calculated results. In the 5- structure, the extra electron goes into the same HOMO and there is almost no change in the orbital spectrum. This is in agreement with the observed $S = {}^1/_2$ ground state as well as the fact that the absorption spectrum is nearly the same as that of the 4- structure. The Hellmann-Feynman force on a cobalt atom differs by only a small amount in the two structures, implying similarly sized structures as is observed in experiment. However, the 5- structure is predicted to be slightly smaller, in contradiction to the crystal data.

Two models were used to extrapolate from the clusters to the mineral cobalt pentlandite. The first was the anion $[Co_8S_6(SH)_8]^{6-}$, in which the cobalt atoms have the same formal charge as in pentlandite. The extra electron goes to fill the highest occupied $12e_u$ level of the 5- structure, and the orbital spectrum is similar to the 4- and 5- clusters. However, the additional electron charge leads to an increase in the inward Hellmann-Feynman force on the cobalt atoms, implying that this oxidation state would tend to be smaller in size. This could be a contribution to the decreased size of the Co_8S_6 core in pentlandite, but does not appear to be the dominant one. Calculations on the $[Co_8(SH)_6(SH)_8]^{2+}$ cluster, in which the extra coordination in the extended material is imitated by additional hydrogen ligands, were also performed. With the 4- cluster as a reference, there is a shifting about of the frontier orbitals, with a stabilization and occupation of what would correspond to the $5e_g$ LUMO of the octahedral cluster. There is also a significant increase in the inward Hellmann-Feynman force on the cobalt atoms relative to the 4- cluster, which is about 4 times that of the 6- cluster. Burdett and Miller also observed such a stabilization in going from the Co_8S_8 to the Co_9S_8 crystal, which corresponds to adding ligands to the bridging sulfurs of the Co_8S_8 material. Their interpretation was that this orbital increases the direct metal-metal interactions to cause the shrinkage. However, it was found here that, although these newly occupied orbitals make a sizable contribution to the increase in the Hellmann-Feynman force, the contribution is nearly identical with that of the orbitals they replace. The decrease in size is therefore due to a subtle combination of effects from the redistribution of the electron charge in the molecule and cannot be associated with only one or a few orbitals. It is clear, though, that the dominant effect on the size of the core is due to extra coordination on the bridging sulfurs.

Acknowledgment. We are grateful to R. H. Holm for suggesting the problem studied in this paper and for helpful discussions during the course of this work. The research was supported in part by a grant from the National Science Foundation. G.G.H. was supported by the Los Alamos National Laboratory during the preparation of the final manuscript.

Vinylidene: The Final Chapter?

Mary M. Gallo, Tracy P. Hamilton, and Henry F. Schaefer III*

Contribution No. 95 from the Center for Computational Quantum Chemistry, University of Georgia, Athens, Georgia 30602. *Received February 21, 1990*

Abstract: Ab initio molecular electronic structure theory is used to study the electronic ground state vinylidene-acetylene isomerization. Vinylidene, acetylene, and the transition state connecting them are located at various levels of theory, including correlated levels, and with large basis sets. The highest level and basis set with which geometry optimizations are performed is the CCSD level with the TZ+2P basis set. These structures are characterized by harmonic vibrational analyses as minima or transition states. Single-point energies also are computed at higher levels of theory, the highest being CCSD/QZ+3P, for all three structures. The effects of carbon atom f functions and hydrogen atom d functions are also explicitly considered. A *classical* barrier to isomerization from vinylidene to acetylene of ~3 kcal/mol is found. The ΔE for isomerization is predicted to be ~43 kcal/mol.

Introduction

Vinylidene, the simplest unsaturated carbene, plays an important role in organic chemistry.[1,2] As a proposed intermediate in many chemical reactions, it has been studied extensively, both experimentally and theoretically. The fundamental issue addressed in these studies has been whether or not vinylidene actually exists as a bound molecule. It has long been established that, *if* vinylidene indeed exists, its lifetime is very short.[3-7] Consequently, it was long believed to be extremely difficult, if not impossible, to observe vinylidene either chemically or spectroscopically.

Some recent experiments have prompted the proposal of vinylidene as an intermediate in chemical reactions[8,9] while others have provided evidence of vinylidene's participation in chemical reactions.[10,11] Field and co-workers[12,13] have very recently observed features diagnostic of vinylidene in the high resolution stimulated emission pumping spectrum of acetylene. By spectral cross correlation and information extracted from the spectrum, they determined an upper bound of 44.4 kcal/mol for the vinylidene zero-point level relative to that of acetylene. However, they were unable to determine the height of the barrier to isomerization of vinylidene to acetylene or even whether or not a barrier exists. Holme and Levine[14] subsequently performed classical trajectory and quantum algebraic computations in order to define the detailed dynamics that produce the spectral structures observed in the stimulated emission pumping spectrum of acetylene. Li-

(1) Stang, P. J. *Acc. Chem. Res.* **1978**, *11*, 107.
(2) Stang, P. J. *Chem. Rev.* **1978**, *78*, 383.
(3) Skell, P. S.; Plonka, J. H. *J. Am. Chem. Soc.* **1970**, *92*, 5620.
(4) Skell, P. S.; Fagone, F. A.; Klabunde, K. J. *J. Am. Chem. Soc.* **1972**, *94*, 7862.
(5) Skell, P. S.; Havel, J. J.; McGlinchey, M. J. *Acc. Chem. Res.* **1973**, *6*, 97.
(6) Reiser, C.; Lussier, F. M.; Jensen, C. C.; Steinfeld, J. I. *J. Am. Chem. Soc.* **1979**, *101*, 350.
(7) Reiser, C.; Steinfeld, J. I. *J. Phys. Chem.* **1980**, *84*, 680.
(8) Davison, P.; Frey, H. M.; Walsh, R. *Chem. Phys. Lett.* **1985**, *120*, 227.
(9) Keifer, J. H.; Mitchell, K. I.; Kern, R. D.; Yong, J. N. *J. Phys. Chem.* **1988**, *92*, 677.
(10) Duran, R. P.; Amorebieta, V. T.; Colussi, A. J. *J. Am. Chem. Soc.* **1987**, *109*, 3154.
(11) Duran, R. P.; Amorebieta, V. T.; Colussi, A. J. *J. Phys. Chem.* **1988**, *92*, 636.
(12) Chen, Y.; Jonas, D. M.; Hamilton, C. E.; Green, P. G.; Kinsey, J. L.; Field, R. W. *Ber. Bunsenges. Phys. Chem.* **1988**, *92*, 329.
(13) Chen, Y.; Jonas, D. M.; Kinsey, J. L.; Field, R. W. *J. Chem. Phys.* **1989**, *91*, 3976.
(14) Holme, T. A.; Levine, R. D. *Chem. Phys.* **1989**, *131*, 169.

0002-7863/90/1512-8714$02.50/0